JOURNAL OF CATALYSIS 84, 8–14 (1983)

Characterization of Molybdenum–Platinum Catalysts Supported on γ-Alumina by X-Ray Photoelectron Spectroscopy

J. E. deVRIES, H. C. YAO, R. J. BAIRD, AND H. S. GANDHI

Engineering and Research Staff, Ford Motor Company, Dearborn, Michigan 48121

Received June 22, 1982; revised June 7, 1983

X-Ray photoelectron spectroscopy (XPS) has been used to investigate the reduction of MoO_3 and MoO_3 + PtO_2 supported on γ-Al_2O_3. Hydrogen reduction of MoO_3/γ-Al_2O_3 at 500°C produced a mixture of Mo(VI), Mo(V), and Mo(IV). Hydrogen reduction of dispersed MoO_3 + PtO_2 on γ-Al_2O_3 showed a similar partial reduction of the Mo(VI) to Mo(V) and Mo(IV) but at significantly lower temperatures than was the case with the supported MoO_3 alone. The extent of the reduction of Mo(VI) increased with the amount of PtO_2 in the samples.

INTRODUCTION

X-ray photoelectron spectroscopy (XPS) has been used previously to investigate the surface chemical properties of supported catalysts (*1–3*). In some instances XPS has been employed to study MoO_3 catalysts related to the hydrodesulfurization process (*4–6*). After hydrogen reduction of MoO_3 supported on γ-Al_2O_3 in the temperature range 400–600°C, Mo(IV), Mo(V), and Mo(VI) have been observed by XPS (*7–8*). The formation of Mo(V) has also been studied by ESR in reduced MoO_3/γ-Al_2O_3 samples (*9*). Temperature Programmed Reduction (TPR) studies of the MoO_3/γ-Al_2O_3 system (*10*) have shown evidence for increased MoO_3-support interaction at low MoO_3 concentrations when the MoO_3 is in the dispersed phase. This interaction at low concentrations has been further studied by XPS, ion scattering, and laser Raman spectroscopies and has been explained by the formation of geometrically coordinated molybdenum "interaction species" on the γ-Al_2O_3 surface (*11*).

In previous studies of PtO_2–MoO_3/γ-Al_2O_3 (*12*) and PtO_2–MoO_3/SiO_2 (*13–14*), it was found that the incorporation of Pt lowers the reduction temperature of MoO_3. TPR data (*12*) show that the presence of PtO_2 lowers the temperature for the first rate maximum of H_2 uptake, suggesting an interaction between PtO_2 and MoO_3. XPS analysis of reduced PtO_2–MoO_3/SiO_2 (*13*) suggests a decrease in the electron density of the Pt atoms in the presence of reduced Mo. This has been interpreted as evidence for direct interaction of the Pt atoms with reduced Mo ions.

The present paper deals with the characterization of both MoO_3 and MoO_3–PtO_2 model supported catalysts by XPS, and a direct comparison of their reduction behavior. The use of a least squares curve fitting routine (*15*) in conjunction with high resolution XPS data has allowed identification of the reduced states of Mo. In addition, the fitting routines have allowed us to make a semi-quantitative measurement of the relative amounts of the various Mo oxidation states.

EXPERIMENTAL

Sample preparation. The MoO_3 samples were prepared by first making a granular support of agglomerated Dispal-M γ-Al_2O_3 powder (Conoco Chemicals). This was accomplished by wetting the powder with water, drying at 120°C and then calcining at 600°C. The solid mass was crushed and sieved to collect the 0.5- to 1.00-mm-diameter fraction (BET area = 150 m^2/g). The granular support was then impregnated

0021-9517/83 $3.00

with an $(NH_4)_2Mo_2O_7$ solution of the desired concentration. The samples were dried at 120°C and then calcined at 400°C. The BET area of the resulting supported MoO_3 sample was 144 m^2/g.

The MoO_3–PtO_2 samples were made by reimpregnating the above Mo-containing γ-Al_2O_3 with an aqueous H_2PtCl_6 solution of desired concentration. The samples were then dried in air at 120°C and finally calcined in air at 500°C. All catalyst compositions are expressed in weight percentage of metal. This sequential impregnation of the Mo oxide and then the noble metal oxide was necessary to prevent the Pt from being unevenly mixed with or covered by the Mo oxide.

It has been determined previously that MoO_3 is present in the dispersed phase for Mo concentrations below (4 μmol Mo)/m^2 (BET) and in a mixture of dispersed and particulate phases for Mo concentrations greater than (4 μmol Mo)/m^2 (BET) (*10*). To study the reduction behavior of a well defined dispersed phase of MoO_3, a concentration of 3.8% Mo was used in the XPS study of the MoO_3 catalyst. This loading on a support of 144 m^2/g (BET) results in a MoO_3 surface concentration of (2.8 μmol Mo)/m^2 (BET) which is within the limit of the dispersed phase. For the study of the $(MoO_3$–$PtO_2)/\gamma$-Al_2O_3 system, loadings of 3.8% Mo with 3.3 or 24% Pt were employed. The samples for the XPS study were prepared by pressing ~400 mg of granular catalyst into a 0.5-mm-thick wafer. The actual sample was then cut from the wafer to fit the sample holder.

X-Ray photoelectron spectroscopy. X-Ray photoelectron spectra were obtained using a Vacuum Generators ESCA 3 electron spectrometer interfaced to a Vacuum Generators 3040 data system. A magnesium anode X-ray source (1253.6 eV) was used to obtain all XPS spectra. The instrumental resolution was 1.1 eV full width at half maximum (FWHM) on the Au($4f_{7/2}$) line. The hydrocarbon contamination C(1*s*) line at 285.0 eV disappeared in most samples after the first reduction, therefore the binding energies of all spectra were referenced to the Al(2*p*) peak of the alumina support at 74.1 eV. This value is in good agreement with other references (*16–18*). All Mo binding energies quoted in this paper pertain to the Mo($3d_{5/2}$) line and are accurate to ±0.1 eV. The Pt binding energies have been compared to standards and literature references (*19, 20*).

After the instrumental vacuum of 1×10^{-9} Torr was reached, the samples were briefly heated to 100°C to remove any adsorbed water. XPS spectra were then recorded before any reduction treatment. All reductions were done with research-grade hydrogen. The hydrogen was backfilled into the system to a partial pressure of 175 Torr. Reductions were carried out for at least 3 h at 300, 400, and 500°C. The reduction temperatures were reached by resistively heating a thin strip of Re foil upon which the catalyst was supported. The surface temperature of the sample was monitored by an infrared pyrometer with an accuracy of ±5°C. All reductions were carried out in a preparation chamber separate from the analyzer chamber. After each reduction the sample was cooled down to room temperature and then the vacuum chamber evacuated so that the XPS spectra might be acquired. No significant changes in the XPS spectra were observed when reductions were carried out longer than three hours.

The least squares curve fitting routine that was employed on the Mo(3*d*) and the combined Al(2*p*)–Pt(4*f*) spectra assumed that all the peaks were Gaussian in shape without an inelastic tail. The spin orbit splitting and peak area ratio of the Mo($3d_{5/2}$) – Mo($3d_{3/2}$) spectra were fixed at 3.2 eV and 1.52, respectively. Both of these parameters were obtained experimentally by analysis of the Mo(3*d*) spectra in the untreated MoO_3/γ-Al_2O_3 samples where only one major component (Mo(VI)) existed. These values are in good agreement with the literature (*8, 21*). There has been a

TABLE 1

Mo Binding Energy Reference Standards

Reference standard	Binding energy (eV)	
	Mo($3d_{5/2}$)	Mo($3d_{3/2}$)
$MoO_3/\gamma\text{-}Al_2O_3$	232.8	236.0
MoO_3	232.6	235.8
MoO_2	229.1	232.3
Mo (metallic)	227.8	231.0

question regarding the value that should be assigned to the Mo(3*d*) FWHM of the supported catalyst. Values in the range of 2.0–2.8 eV have been quoted by a number of authors (*5, 8, 11*). The values used in this work were determined experimentally in the same manner as the Mo(3*d*) peak area ratio and peak separation values. The FWHM value for the 3.8% Mo was determined to be 2.6 eV. This value was also fixed in the least squares fit. In addition, the Pt($4f_{7/2}$)–Pt($4f_{5/2}$) spin orbit splitting and peak area ratio were also determined experimentally along with the Pt(4*f*) and Al(2*p*) FWHM.

RESULTS AND DISCUSSION

$MoO_3/\gamma\text{-}Al_2O_3$ Samples

To provide a basis for the interpretation of the XPS spectra, a number of Mo reference standards were analyzed and the results are shown in Table 1. The spectrum from an untreated supported 3.8% Mo sample showed a single Mo($3d_{5/2}$) component at 232.8 eV corresponding to Mo(VI).

When the 3.8% Mo sample was reduced at 300°C it remained predominantly Mo(VI) (232.7 eV), and a considerably smaller component was observed at 230.8 eV which can be assigned to Mo(V). This spectrum is shown in Fig. 1a. After 3 h at 400°C in H_2, more reduction to Mo(V) is observed along with the emergence of a lower oxidation state at 228.8 eV which can be attributed to Mo(IV). This spectrum, which is similar to that reported by Jagannathan *et al.* (*8*) is

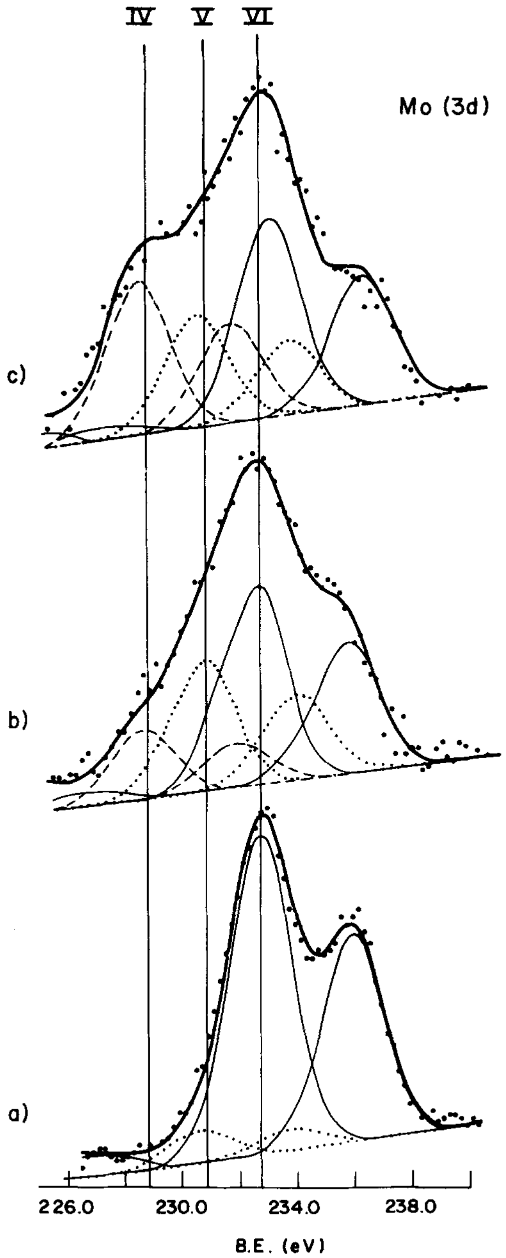

FIG. 1. Mo(3*d*) XPS spectra of 3.8% Mo (a) after 3 h in H_2 at 300°C, (b) after 3 h in H_2 at 400°C, (c) after 3 h in H_2 at 500°C. The bold dots represent the acquired data, the thick solid lines represent the least squares fit, the thin solid lines represent the fitted Mo(VI) state, the light dotted lines represent the fitted Mo(V) state, and the dashed lines represent the fitted Mo(IV) state.

shown in Fig. 1b. Further reduction at 500°C shows an increase in the relative amount of Mo(IV) as seen in Fig. 1c. However, the strong shoulder at 235.9 eV which is due to the Mo(VI) $3d_{3/2}$ peak shows that some Mo(VI) remains on the surface.

In contrast to the results of this paper and the results of a number of other authors (*5, 7, 8*) which suggests incomplete reduction of the Mo(VI) to Mo(V) and Mo(IV), Zingg *et al.* (*11*) reported complete reduction of the Mo(VI) to Mo(V) and Mo(IV). In an attempt to explain this discrepancy, Zingg reworked Patterson's data (*5*) and showed that a two component treatment (Mo(IV) and Mo(V)) of the data resulted in a better statistical fit and a more reasonable FWHM for the Mo(3*d*) peaks (2.8 vs 2.1 eV). When this method of fitting was applied to the data presented here, a poorer statistical fit and an unrealistic FWHM of 3.3 eV was obtained. This unrealistic FWHM was to be expected since the envelope of the Mo(3*d*) region is ~10.1 eV wide in our data vs ~8.2 eV in Patterson's data. The difference in width cannot be attributed to differences in resolution or charging since the width of the Al(2*p*) peak was found to be 3.0 eV FWHM which is comparable to the width observed by Zingg. Therefore the difference in the results lies in the experiments and not in the data analysis.

The significant difference between the experiments is that our reductions were carried out at relatively low H_2 pressure (175 Torr) in a static system as opposed to the 1-atm flow reactor used by Zingg and by Patterson. The lower H_2 pressure might in itself contribute to the incomplete reduction of the sample. Also, Massoth (*22*) has proposed that a gaseous layer of water vapor surrounds the catalyst particles in a static system, and that the existence of this layer might result in incomplete reduction by the reoxidation of the sample. In any case these results provide a baseline for direct comparison of hydrogen reduction in our system of Mo alone, with MoO_3–PtO_2 samples.

MoO_3 + PtO_2/γ-Al_2O_3 Catalyst

In this section two MoO_3–PtO_2 samples, one of high Pt loading (3.8% Mo/24% Pt) and one of low Pt loading (3.8% Mo/3.3% Pt), are compared to a 3.8% MoO_3 sample. The Mo(3*d*) XPS spectrum of all three untreated samples consisted of a single doublet in which the Mo($3d_{5/2}$) binding energy appeared at 232.8 eV. This binding energy corresponds to a Mo(VI) state. There was no difference observed in the three spectra acquired before any reduction treatment.

Figure 2 represents the Mo(3*d*) spectra of the two MoO_3–PtO_2 samples and the 3.8% MoO_3 alone after 3 h in H_2 at 300°C. As in the previous section the 3.8% Mo spectrum (Fig. 2a) shows a partial reduction of the Mo(VI) to only Mo(V). In contrast, spectra from both MoO_3–PtO_2 samples show significant reduction to both Mo(IV) and Mo(V), with some Mo(VI) remaining. Comparison of the low and high concentrations of Pt, Figs. 2b and c, respectively, reveals that more reduction to Mo(IV) occurs on the 24% Pt sample. These results correlate well with the TPR results of Gandhi *et al.* (*12*) where it was reported that the presence of PtO_2 in the MoO_3–PtO_2 catalyst lowered the temperature of the first rate maximum of the H_2 uptake from 450°C to 250, 160, or 100°C depending on the concentration of PtO_2 on the sample surface.

The Pt(4*f*)–Al(2*p*) spectra of the 3.8% Mo/24.0% Pt sample before and after the 300°C reduction are shown in Fig. 3. The Al(2*p*) masks reliable detection of the Pt(4*f*) in the 3.8% Mo/3.3% Pt sample and therefore only spectra from the higher Pt loading (24%) are presented. The binding energy of the Pt($4f_{7/2}$) peak before reduction as seen in Fig. 3a is 72.4 eV which is too low to correspond to either PtO or PtO_2 but might be a suboxide species produced during the heating to 100°C. The oxidized Pt species (B.E. 71.5–72.0 eV) observed by Ermakov (*13*) after 300°C reduction were not observed in our work, rather the Pt, as seen in Fig. 3b, immediately converted to a metallic state

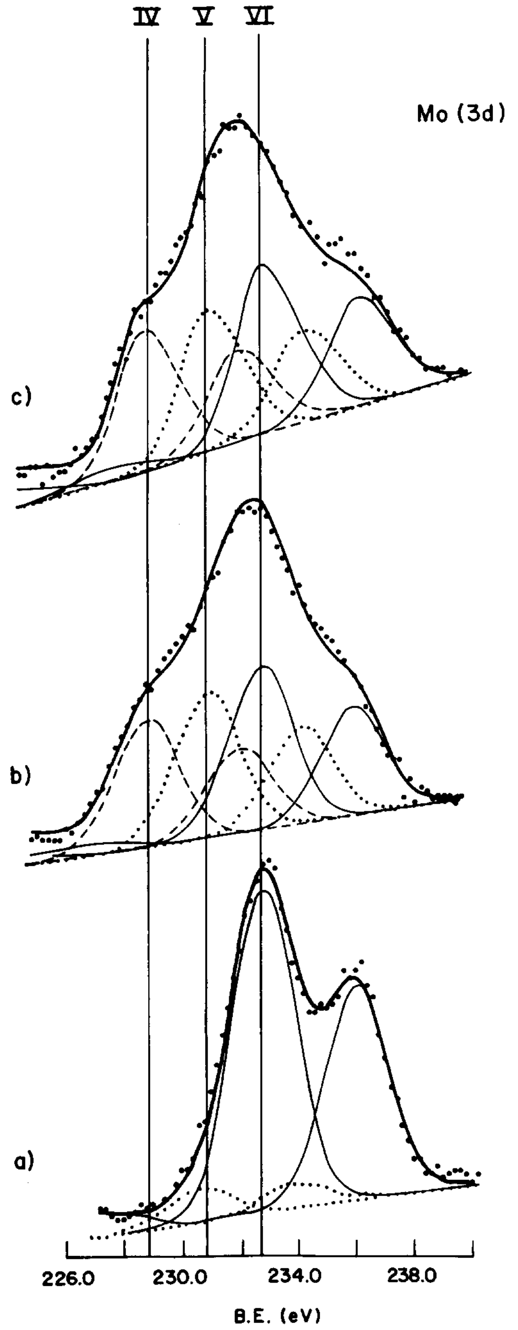

FIG. 2. Mo(3*d*) XPS spectra after 3 h in H_2 at 300°C (a) 3.8% Mo, (b) 3.8% Mo/3.3% Pt, (c) 3.8% Mo/24.0% Pt (symbols as in Fig. 1).

(B.E. 70.9 eV) after reduction. The reduction of Pt at 300°C substantiates the conclusion by Gandhi *et al.* that the rate maximum for the reduction of PtO_2 must coincide with the aforementioned first rate maximum of the Mo(VI). Samples containing only supported PtO_2 were also analyzed, and the Pt states before and after H_2 reduction were identical to that of the MoO_3–PtO_2 system. This difference in the observed behavior of the Pt between this work and that of Ermakov, may reflect the substantial difference in the Pt loadings or a

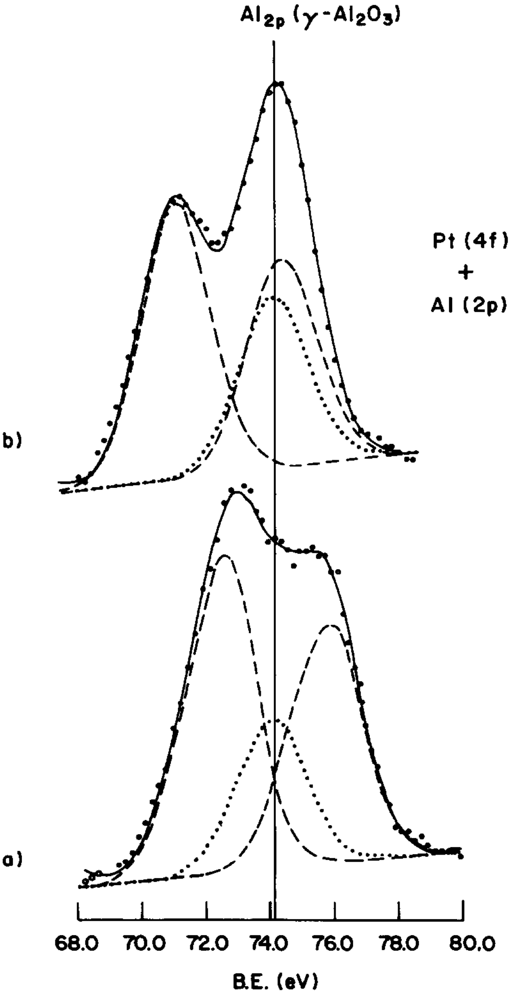

FIG. 3. Al(2*p*)–Pt(4*f*) spectra of the 3.8% Mo/24.0% Pt sample (a) before treatment, (b) after 3 h in H_2 at 300°C. For the Al(2*p*)–Pt(4*f*) spectra the open circles represent the acquired data, the solid lines represent the least squares fit, the dotted lines represent the γ-Al_2O_3 Al(2*p*) peak at 74.1 eV, and the dashed lines represent the Pt(4*f*) peaks.

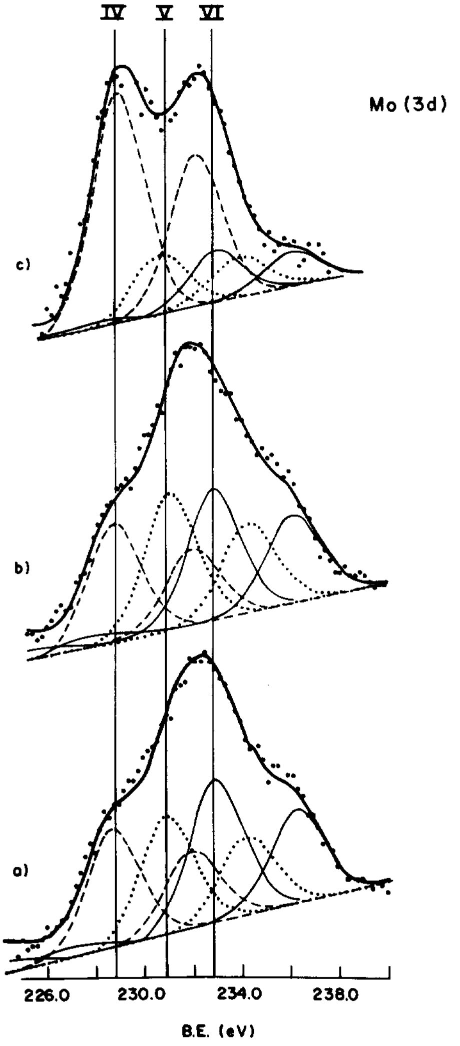

FIG. 4. Mo(3*d*) spectra after 3 h in H_2 at 500°C (a) 3.8% Mo, (b) 3.8% Mo/3.3% Pt, (c) 3.8% Mo/24.0% Pt (symbols as in Fig. 1).

difference between the SiO_2 and the γ-Al_2O_3 supports. The Pt(4*f*) spectra at higher reduction temperatures are identical to Fig. 3b.

There is little change observed in the XPS spectrum of the sample with low Pt loading after further reduction at 400 and 500°C. Figure 4 compares the XPS Mo(3*d*) spectra taken from all three samples after the 500°C reduction treatment. Close observation of the spectra from the 3.8% Mo and the 3.8% Mo/3.3% Pt sample, Figs. 4a and b, respectively, reveal no significant differences in these spectra. The 3.3% Pt XPS results and the previous TPR study (*12*) are in agreement that the presence of Pt only lowers the temperature for that reduction which occurs below 500°C. This reduction has been associated with the removal of the capping oxygen atoms of Mo (*12*).

The 24% Pt catalyst on the other hand shows continued reduction to a comparatively higher concentration of Mo(IV) at 500°C as seen in Fig. 4c. This continued reduction may be due to a number of reasons. The relatively high amount of Pt (24%) may be competing for interaction sites on the γ-Al_2O_3 surface decreasing the amount of strongly interacted Mo species. This would result in greater reduction of the Mo(VI) to Mo(IV), as was reported by Zingg for high MoO_3 loadings (*11*). Also, the gaseous layer of water surrounding the catalyst particles in a static system as proposed by Massoth (*22*) might reoxidize the Mo(IV) and (V) and thereby establish a pseudo-equilibrium state. This state may be altered by a higher Pt/Mo ratio inhibiting the reoxidation of the reduced Mo species. This could explain not only the increased reduction of the 24% Pt sample at 500°C but also the greater reduction of the Pt containing sample at 300°C as seen in Fig. 3b.

SUMMARY

XPS used in conjunction with a curve-fitting procedure has allowed explicit definition of the reduced chemical states of γ-Al_2O_3 supported MoO_3 and MoO_3–PtO_2 model catalysts. In the MoO_3 samples Mo(VI), (V), and (IV) coexist after reduction at temperatures less than 500°C. Addition of PtO_2 to the MoO_3 catalysts lowers the temperature for the initial reduction of Mo(VI) below 300°C. Higher loadings of Pt in the MoO_3–PtO_2 system result in greater reduction of the Mo at the same temperatures.

REFERENCES

1. Edmonds, T., and Mitchell, P. C. H., *J. Catal.* **64,** 491 (1980).
2. Okamoto, Y., Imanaka, T., and Teranishi, S., *J. Catal.* **65,** 448 (1980).
3. Kerkhof, F. P. J. M., and Moulijn, J. A., *J. Phys. Chem.* **83,** 1812 (1979).
4. Okamoto, Y., Nakano, H., Shimokawa, T., Imanaka, T., and Teranishi, S., *J. Catal.* **50,** 447 (1977).
5. Patterson, T. A., Carver, J. C., Leyden, D. E., and Hercules, D. M., *J. Phys. Chem.* **80,** 1700 (1975).
6. Declerck-Grimee, R. I., Canesson, P., Friedman, R. M., and Fripiat, J. J., *J. Phys. Chem.* **82,** 885 (1978).
7. Cimino, A., and De Angelis, B. A., *J. Catal.* **36,** 11 (1975).
8. Jagannathan, K., Srinivasan, A., and Rao, C. N. R., *J. Catal.* **69,** 418 (1981).
9. Seshadri, K. S., and Petrakis, L., *J. Catal.* **30,** 195 (1973).
10. Yao, H. C., *J. Catal.* **70,** 440 (1981).
11. Zingg, D. S., Makovsky, L. E., Tischer, R. E., Brown, F. R., and Hercules, D. M., *J. Phys. Chem.* **84,** 2898 (1980).
12. Gandhi, H. S., Yao, H. C., and Stepien, H. K., "Catalysis Under Transition Conditions," p. 144. ACS Symposium Series, No. 178, 1982.
13. Ermakov, Yu. I., Ioffe, M. S., Ryndin, Yu. A., and Kuznetsov, B. N., *Kinet. Katal.* **16,** 807 (1975).
14. Ermakov, Yu. I., Kuznetsov, B. N., Ryndin, Yu. A., and Duplyakin, V., *Kinet. Katal.* **15,** 1093 (1974).
15. Fadley, C. S., PHd thesis, University of California at Berkeley, 1970 (LBL Report UCRL-19535 1970).
16. Ogilvie, J. L., and Wolberg, A., *Appl. Spectrosc.* **26,** 402 (1976).
17. Madey, T. E., Wagner, C. D., and Joshi, A., *J. Electron. Spectrosc.* **10,** 359 (1977).
18. Ng, K. T., and Hercules, D. M., *J. Phys. Chem.* **80,** 2095 (1977).
19. Escard, J., Pontvianne, P., and Contour, J. P., *J. Electron Spectrosc.* **6,** 17 (1975).
20. Kim, K. S., Winograd, N., and Davis, R. E., *J. Am. Chem. Soc.* **93,** 6296 (1971).
21. Gajardo, P., Pirotte, D., Defosse, C., Grange, P., and Delmon, B., *J. Electron Spectrosc. Relat. Phenom.* **17,** 121 (1979).
22. Massoth, F. E., *J. Catal.* **54,** 450 (1978).